



# Slowing sub-picosecond laser pulses with 0.55 mm-thick cholesteric liquid crystal

CHUN-WEI CHEN,<sup>1</sup> XUOXUE GUO,<sup>1</sup> XINGJIE NI,<sup>1</sup> TSUNG-HSIEN LIN,<sup>2</sup> AND IAM CHOON KHOO<sup>1,\*</sup>

<sup>1</sup>Department of Electrical Engineering, Pennsylvania State University, University Park, PA 16802, USA

<sup>2</sup>Department of Photonics, National Sun Yat-sen University, Kaohsiung, Taiwan

\*ick1@psu.edu

**Abstract:** Extraordinarily thick well-aligned planar cholesteric liquid crystal (CLC) cells with low scattering loss have been successfully fabricated using a *field-assisted self-assembly technique*. These cells exhibit excellent 1D photonic crystal properties such as photonic band-gap and strong group velocity dispersion at the band edges and enable several all-optical ultrafast laser pulse modulation operations. In particular, we report an experimental observation of the clear separation of  $\sim 1$  ps between the normal and slow 600 fs light pulses after traversing a 0.55 mm-thick CLC. With simple optimization procedures, such as tuning the photonic band-edge and laser wavelength, and use of more appropriate laser pulse duration and bandwidth, one could realize a much larger effect. These extraordinarily thick CLCs have previously also demonstrated their capabilities for direct compression, stretching and recompression of sub-picosecond pulses, and thus present themselves as promising compact, all-optical and versatile alternatives to existing materials for slow-light production and ultrafast pulse modulation operations.

© 2017 Optical Society of America

**OCIS codes:** (160.3710) Liquid crystals; (160.5298) Photonic crystals; (320.7080) Ultrafast devices.

## References

1. I. C. Khoo and S.-T. Wu, *Optics and Nonlinear Optics of Liquid Crystals* (World Scientific Publishing, 1995).
2. I. C. Khoo, "Nonlinear optics of liquid crystalline materials," *Phys. Rep.* **471**(5-6), 221–267 (2009).
3. I. C. Khoo, "Nonlinear optics, active plasmonics and metamaterials with liquid crystals," *Prog. Quantum Electron.* **38**(2), 77–117 (2014).
4. J. Ptasinski, S. W. Kim, L. Pang, I. C. Khoo, and Y. Fainman, "Optical tuning of silicon photonic structures with nematic liquid crystal claddings," *Opt. Lett.* **38**(12), 2008–2010 (2013).
5. C.-Y. Wang, C.-W. Chen, H.-C. Jau, C.-C. Li, C. Y. Cheng, C. T. Wang, S. E. Leng, I. C. Khoo, and T. H. Lin, "All-optical transistor- and diode-action and logic gates based on anisotropic nonlinear responsive liquid crystal," *Sci. Rep.* **6**(1), 30873 (2016).
6. I. C. Khoo, C.-W. Chen, and T.-J. Ho, "High efficiency holographic Bragg grating with optically prolonged memory," *Sci. Rep.* **6**(1), 36148 (2016).
7. Z.-G. Zheng, Y. Li, H. K. Bisoyi, L. Wang, T. J. Bunning, and Q. Li, "Three-dimensional control of the helical axis of a chiral nematic liquid crystal by light," *Nature* **531**(7594), 352–356 (2016).
8. T. J. White, M. E. McConney, and T. J. Bunning, "Dynamic color in stimuli-responsive cholesteric liquid crystals," *J. Mater. Chem.* **20**(44), 9832–9847 (2010).
9. S. D. Jacobs, K. A. Cerqua, K. L. Marshall, A. Schmid, M. J. Guardalben, and K. J. Skerrett, "Liquid-crystal laser optics: design, fabrication, and performance," *J. Opt. Soc. Am. B* **5**(9), 1962–1979 (1988).
10. N. Y. Ha, Y. Ohtsuka, S. M. Jeong, S. Nishimura, G. Suzuki, Y. Takanishi, K. Ishikawa, and H. Takezoe, "Fabrication of a simultaneous red-green-blue reflector using single-pitched cholesteric liquid crystals," *Nat. Mater.* **7**(1), 43–47 (2008).
11. T. J. White, R. L. Bricker, L. V. Natarajan, N. V. Tabiryan, L. Green, Q. Li, and T. J. Bunning, "Phototunable azobenzene cholesteric liquid crystals with 2000 nm range," *Adv. Funct. Mater.* **19**(21), 3484–3488 (2009).
12. L. Cattaneo, M. Savoini, I. Mušević, A. Kimel, and T. Rasing, "Ultrafast all-optical response of a nematic liquid crystal," *Opt. Express* **23**(11), 14010–14017 (2015).
13. J. Hwang, N. Y. Ha, H. J. Chang, B. Park, and J. W. Wu, "Enhanced optical nonlinearity near the photonic bandgap edges of a cholesteric liquid crystal," *Opt. Lett.* **29**(22), 2644–2646 (2004).
14. L. Song, S. Fu, Y. Liu, J. Zhou, V. G. Chigrinov, and I. C. Khoo, "Direct femtosecond pulse compression with miniature-sized Bragg cholesteric liquid crystal," *Opt. Lett.* **38**(23), 5040–5042 (2013).
15. N. Sanner, N. Huot, E. Audouard, C. Larat, J.-P. Huignard, and B. Loiseaux, "Programmable focal spot shaping of amplified femtosecond laser pulses," *Opt. Lett.* **30**(12), 1479–1481 (2005).

16. A. Jullien, U. Bortolozzo, S. Grabielle, J.-P. Huignard, N. Forget, and S. Residori, "Continuously tunable femtosecond delay-line based on liquid crystal cells," *Opt. Express* **24**(13), 14483–14493 (2016).
17. Y. Liu, Y. Wu, C.-W. Chen, J. Zhou, T. H. Lin, and I. C. Khoo, "Ultrafast pulse compression, stretching-and-recompression using cholesteric liquid crystals," *Opt. Express* **24**(10), 10458–10465 (2016).
18. F. Xia, L. Sekaric, and Y. Vlasov, "Ultracompact optical buffers on a silicon chip," *Nat. Photonics* **1**(1), 65–71 (2007).
19. P. Colman, C. Husko, S. Combr  , I. Sagnes, C. W. Wong, and A. De Rossi, "Temporal solitons and pulse compression in photonic crystal waveguides," *Nat. Photonics* **4**(12), 862–868 (2010).
20. T. Baba, "Slow light in photonic crystals," *Nat. Photonics* **2**(8), 465–473 (2008).
21. C. Monat, M. de Sterke, and B. J. Eggleton, "Slow light enhanced nonlinear optics in periodic structures," *J. Opt.* **12**(10), 104003 (2010).
22. J. T. Mok, C. Martijn de Sterke, I. C. M. Littler, and B. J. Eggleton, "Dispersionless slow light using gap solitons," *Nat. Phys.* **2**(11), 775–780 (2006).
23. K. S. Abedin, G.-W. Lu, and T. Miyazaki, "Slow light generation in singlemode Er-doped tellurite fibre," *Electron. Lett.* **44**(1), 16–17 (2008).
24. C.-J. Ma, L.-Y. Ren, Y.-P. Xu, Y.-L. Wang, H. Zhou, H.-W. Fu, and J. Wen, "Theoretical and experimental study of structural slow light in a microfiber coil resonator," *Appl. Opt.* **54**(18), 5619–5623 (2015).
25. M. S. Bigelow, N. N. Lepeshkin, and R. W. Boyd, "Observation of ultraslow light propagation in a ruby crystal at room temperature," *Phys. Rev. Lett.* **90**(11), 113903 (2003).
26. Y. Okawachi, M. S. Bigelow, J. E. Sharping, Z. Zhu, A. Schweinsberg, D. J. Gauthier, R. W. Boyd, and A. L. Gaeta, "Tunable all-optical delays via Brillouin slow light in an optical fiber," *Phys. Rev. Lett.* **94**(15), 153902 (2005).
27. M. D. Lukin and A. Imamog  lu, "Controlling photons using electromagnetically induced transparency," *Nature* **413**(6853), 273–276 (2001).
28. P. J. Bustard, K. Heshami, D. G. England, M. Spanner, and B. J. Sussman, "Raman-induced slow-light delay of THz-bandwidth pulses," *Phys. Rev. A* **93**(4), 043810 (2016).
29. Y. A. Vlasov, M. O'Boyle, H. F. Hamann, and S. J. McNab, "Active control of slow light on a chip with photonic crystal waveguides," *Nature* **438**(7064), 65–69 (2005).
30. P.-C. Ku, F. Sedgwick, C. J. Chang-Hasnain, P. Palinginis, T. Li, H. Wang, S.-W. Chang, and S.-L. Chuang, "Slow light in semiconductor quantum wells," *Opt. Lett.* **29**(19), 2291–2293 (2004).
31. K. W. DeLong, R. Trebino, J. Hunter, and W. E. White, "Frequency-resolved optical gating with the use of second-harmonic generation," *J. Opt. Soc. Am. B* **11**(11), 2206–2215 (1994).

## 1. Introduction

Liquid crystals in their ordered mesophases, particularly nematic and cholesterics (including cholesteric blue-phase) possess many unique material and optical properties for photonic applications. In particular, the extraordinarily large birefringence of nematics and the easy susceptibility of the crystalline axis to external fields have been utilized in a wide assortment of electro-optic and nonlinear optical devices [1–11]. The underlying mechanisms for field induced birefringence or index changes are characteristically slow, and therefore most photonic applications such as tunable filters, switches and ubiquitous display devices generally do not involve ultrafast (femtoseconds) laser pulses. Several recent works [12–17], however, have demonstrated that liquid crystals are also capable of modulating ultrafast laser pulses. In particular, cascaded nematic liquid crystals have been employed to impart electronically tunable delay and phase shifts on femtosecond pulses [16], while [14, 17] have demonstrated the feasibility of all-optical direct compression, stretching and recompression of 100 fs – 850 fs pulses. In the context of ultrafast laser pulse modulation, another interesting and useful effect is to slow the group velocity of light. Many mechanisms and optical schemes have been investigated and shown to be highly effective to generate slow light [18–30] with some exhibiting impressively slow light velocity. Nevertheless, the requirements to produce slow light such as tuning the laser frequency to exact resonance with particular atomic transition, proper balance of nonlinearity with dispersion in specialized guided wave geometry over long distances...etc., in addition to having to incorporate bulky/cumbersome optics, place severe limitations on their practical implementation. It is therefore highly desirable to seek and develop alternative materials that would overcome these limitations and enable compact and versatile direct-action device with a broad operating spectral coverage.

In this paper, we report experimental observation of group velocity slowing down of sub-picosecond (650 fs) laser pulses with a 0.55 mm thick cholesteric liquid crystal (CLC) cell. In

a preliminary feasibility demonstration, a 1 ps separation between normal and slow light is obtained without optimization. CLC comprises conventional nematic and a chiral agent; in the ordered phase, the constituent molecules self-assemble in a spiral with a pitch determined by the concentration of the chiral agent, *cf.* Fig. 1(a). Due to the birefringence  $\Delta n = n_e - n_o$  (where  $n_e$  is the index for light polarization along the director axis and  $n_o$  for light polarization perpendicular to the axis), a CLC is optically a 1D photonic crystal and exhibits typical photonic crystal properties such as photonic bandgap and strong dispersions near the band-edges, *cf.* Fig. 1(b), for circularly polarized light. Therefore, if a linearly polarized light pulse (wavelength located near the band-edge) is incident on the cell, one of its two circularly polarized components ‘experiences’ the photonic crystal properties and propagates at a slower speed due to band-edge dispersion, while the other simply propagates with normal light velocity. If the propagation distance, *i.e.* thickness of the cell is sufficiently large, these two circularly polarized light pulses of different handedness will emerge separately.

To estimate the required thickness for measurable pulse separation, we note here that at light speed  $c$ , the transit time through 300  $\mu\text{m}$  in air ( $n \approx 1$ ) is 1 ps. On the other hand, typical liquid crystal cell (index  $n \approx 1.5$ ) thickness is on the order of 10  $\mu\text{m}$ , corresponding to a transit time of  $\sim 50$  fs. Therefore, unless the laser pulse is very short ( $< 50$  fs) and the slow-down is very substantial, it is very difficult to obtain measurable time delay between the slow and the normal light. For longer pulses, *e.g.* 650 fs used in this study, the first requirement is therefore a record-setting CLC thickness measuring in 100’s micron. This as well as other requirements for ultrafast pulse modulations [17] prompted our development of the Field-Assisted-Self-Assembly (FASA) technique to fabricate such extraordinarily thick CLC cells.

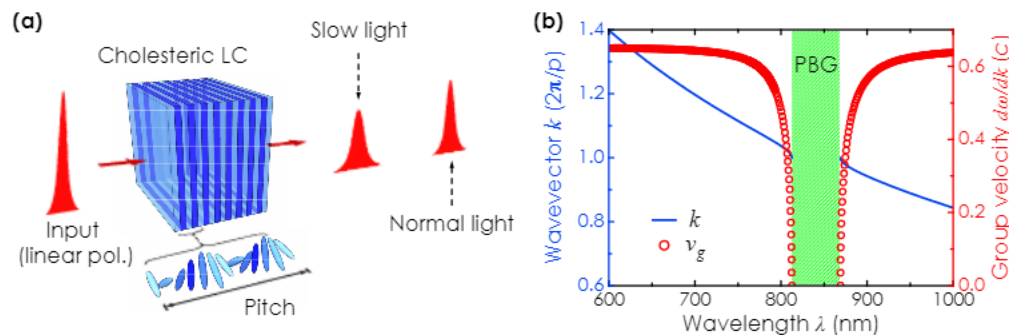


Fig. 1. (a) Schematic depiction of a cholesteric liquid crystal cell (CLC) that exhibits 1D photonic crystal (Bragg grating) properties suitable for self-action femtoseconds laser pulse modulation without additional optics. (b) Plots of group velocity  $d\omega/dk$  and wavevector  $k$  as function of the optical wavelength in the vicinity of the photonic bandgap showing the dramatic changes in group velocity near the band edges based on an *ideal* CLC with  $n_o = 1.4839$ ,  $n_e = 1.5872$ , and  $p = 547.6$  nm.

## 2. Field-assisted self-assembly (FASA) of $\sim\text{mm}$ thick CLC

Conventional CLC cells of thickness ( $d$ ) in the few microns to at most 10’s  $\mu\text{m}$  scale rely on self-assembly of cholesteric mixture molecules between two surfaces coated with planar-alignment layer. The pitch ( $p$ ) characterizing the spiral of director axis from one surface to the other for optical application is on the order of 500 nm (0.5  $\mu\text{m}$ )–1000 nm (1  $\mu\text{m}$ ). Thus, the thickness-to-pitch ratio  $d/p$  is at most  $\sim 100$  and good planar CLC cells can be achieved with the surface anchoring forces. However, in thicker cells, the influence of surface-alignment layers on the bulk LC molecules becomes weaker, and invariably results in highly scattering focal conic texture, *cf.* Fig. 2(a). In our FASA fabrication technique illustrated in Figs. 2(b)–2(d), the departure of the director axis spiral-direction from cell window normal (*i.e.* director axis in planar alignment) during the molecular assembly process is avoided by using a nematic constituent with negative dielectric anisotropy, and employing a strong AC field

applied across the ITO-coated cell windows to enforce planar alignment. The empty cell is made of two flat windows with the inner surfaces coated with Indium Tin Oxide (ITO) to act as transparent electrodes, and rubbed polyimide as planar-alignment layers, with non-coated 550  $\mu\text{m}$  thick glass slides acting as spacers. The polyimide layers are rubbed to define the LC director orientation on the substrate surfaces. The cell is then filled with the CLC mixture in the isotropic phase, Fig. 2(b). As the sample is allowed to cool down to room temperature naturally [cooling rate  $\sim$  a few  $^{\circ}\text{C}/\text{min}$  with ambient temperature of 25  $^{\circ}\text{C}$ ], an AC electric field derived from a voltage source ( $\sim$ 2500 V; 1 kHz; rectangular) is applied across the cell window for an extended period of  $\sim$ 12 hours while the mixture sits at room temperature, cf. Figs. 2(c) and 2(d).

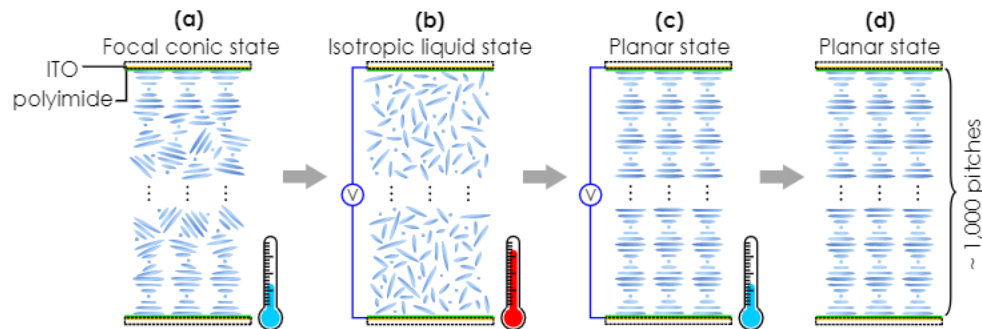


Fig. 2. (a) CLC with focal conic structure as a result of director axis deviating from planar alignment. (b) Random orientation of director axis in the isotropic liquid phase; AC voltage begins. (c) Sample cooling down to ordered phase; AC field enforces planar alignment initiated by surface anchoring forces. (d) AC field removed after  $\sim$ 12 hours at room temperature.

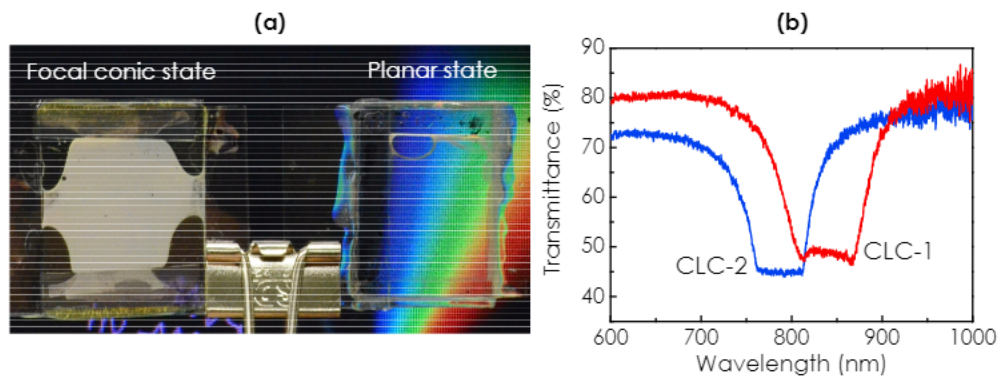


Fig. 3. (a) Photograph of two CLC cells on top of some color background. [Left] Highly scattering (opaque) 200  $\mu\text{m}$  thick focal conic texture by conventional self-assembly; [Right] Transparent (low-scattering) planar CLC cell fabricated with the field assisted self-assembly (FASA) technique. (b) Typical transmission spectra of randomly polarized light at normal incidence of two 550  $\mu\text{m}$  thick planar CLC cells made with the FASA technique showing the photonic bandgap experienced by the left circularly polarized (LHCP) component; loss far away from the band edges is due mainly to reflections from uncoated cells surfaces.

Several negative dielectric nematic compounds and chiral agents from a variety of sources have been tested, and they all yield well aligned samples with thicknesses up to  $\sim$ 550  $\mu\text{m}$ . The nematic constituent used is characterized by the following material properties:  $n_e = 1.5872$ ,  $n_o = 1.4839$ , and  $\Delta\epsilon = -3.6$  with a nearly 100 $^{\circ}\text{C}$  nematic temperature range. The chiral agent used is S5011 [Helical twisting power  $> 100 \mu\text{m}^{-1}$  from Jiangsu Hecheng Display Technology Co. Ltd]. For making CLC cells with pitches of around  $\sim$ 510–545 nm and bandgaps/edges in the 800 nm region, the concentrations used for the chiral agent and the nematic constituent are



~1.6 wt% and ~98.4 wt%, respectively. Using slightly different concentrations of the chiral agent, one can tune the location of the photonic bandgap/band-edges, as exemplified by CLC-1 and CLC-2. In comparison with samples made with conventional self-assembly method that yield very high scattering focal conic textures, cells fabricated with the *FASA* procedure are found to exhibit uniform planar alignment and consequently almost negligible scattering loss, c.f. Figure 3 (a), and well defined photonic bandgap in their transmission spectra, c.f. Figure 3(b) for two 550  $\mu\text{m}$  thick CLC samples fabricated with FASA technique. The CLC planar texture remains intact indefinitely.

### 3. Slow light experiment

Using these extraordinarily thick CLC cells, we have observed to our knowledge for the first time a clear separation between normal and slow light. The experimental setup is shown in Fig. 4. The *linearly polarized laser pulse train* originating from a femtosecond laser system (repetition rate: 80 MHz; pulse duration: 140 fs; wavelength: 800 nm; maximum power: 200 mW) is first spectrally dispersed and divided, and then reconstituted to yield two pulse trains, one providing gate pulses and the other (the probe pulses) is incident on the sample under study. The resulting individual laser pulse duration in air is measured to be 650 fs, with a bandwidth of ~7 nm.

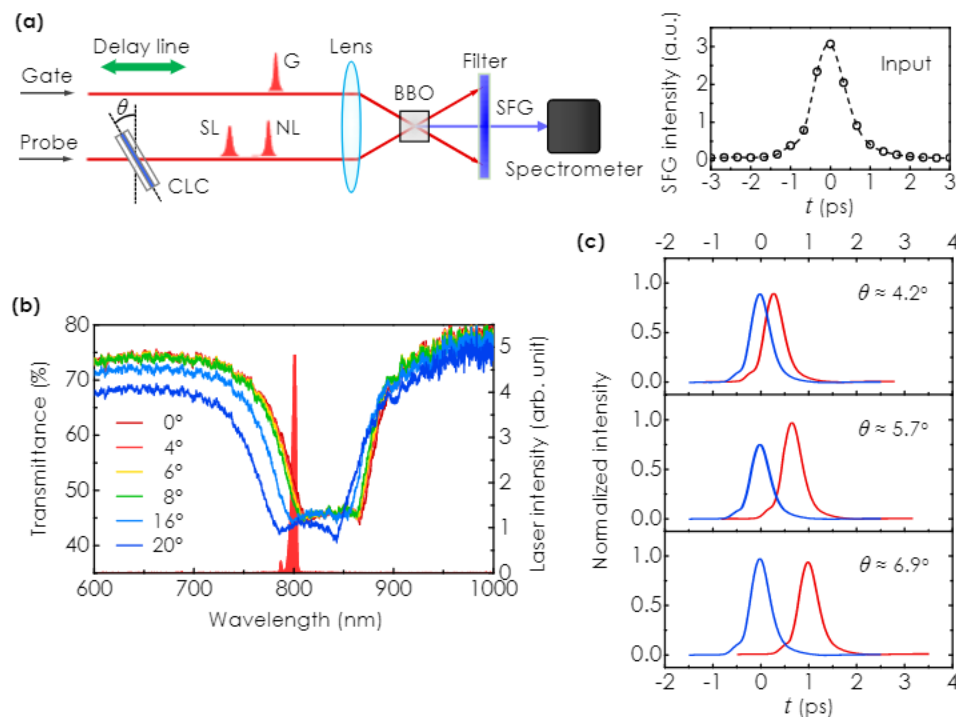


Fig. 4. (a) Experimental setup for measuring slow-down of linearly polarized 650 fs laser pulses by the CLC-1 cell. Note that the SFG signal detected by the spectrometer can be generated only if the gate and probe pulses overlap spatially. NL: normal light; SL: slow light; BBO: beta barium borate crystal for SFG. Insert on the right hand side depicts typical SFG signal for a 650 fs probe pulse. (b) Transmission spectrum of CLC-1 as a function of the tilt angle. The photonic bandgap shifts towards the short wavelength region so that the laser wavelength is located closer to the band edge. (c) Exit normal (blue) and slow (red) light pulses extracted from the SFG signal for the case when the CLC-1 cell is tilted at increasing angle  $\theta$  away from the normal direction.

Measurement of the pulse duration is performed by a home-made system based on sum frequency generation (SFG) akin to Second Harmonic Frequency-Resolved Optical Gating

technique (SH-FROG) [31]. The system essentially measures the temporal characteristics of the exit light from the sample (CLC cell) by overlapping it with the gate pulse. The sum-frequency-generation (SFG) intensity from the BBO crystal is monitored as a function of the delay of the gate pulse, and therefore the temporal overlapping between the output pulses and the gate pulse can be quantified. As shown in Fig. 4(a) insert, the observed SFG signal ( $\sim 1.3$  ps wide) is about twice as broad as the actual pulse duration (650 fs). Using this as a rough guide, the temporal characteristics of exit laser pulses from the CLC cell can be deduced.

Since the operating laser wavelength is 800 nm with a bandwidth of  $\sim 7$  nm, for band-edge dispersion effect, we use CLC-1 cell whose short wavelength band-edge is located at 812.5 nm, c.f. Figure 3(b) and 4(b). It is then inserted in the path of the probe pulse, and the generated SFG signal is monitored as a function of the time delay. At normal incidence ( $\theta = 0$ ), owing to the large detuning from the band-edge, the output consists of a single pulse of  $\sim 650$  fs duration, indicating no separation between the slow light (SL) and the normal light (NL). By tilting the CLC cell from the normal-incidence direction, the band-edge is blue-shifted to be closer to the laser wavelength, cf. Fig. 4(b). Pulse separation begins to manifest at a tilt angle  $\theta \approx 4.2^\circ$ , and becomes more pronounced for larger tilt angle; at  $\theta \approx 6.9^\circ$ , we detected a pulse separation of over 1 ps. A quantitative analysis of the actual propagation through a highly dispersive photonic crystal near the band-edge is quite complex. Qualitatively, the right-handed circularly polarized (RHCP) pulse that does not ‘see’ the photonic band structure would simply propagate as normal light at a group velocity  $v_g = c/n$ , where  $n = (n_o + n_e)/2 \approx 1.53$ , with a transit time  $\tau_{NL} = L/v_{NL} \sim 2.81$  ps for  $L = 0.55$  mm. On the other hand, the left-hand circularly polarized component (LHCP) ‘experiences’ the band-edge dispersion and propagates as the slow light with a group velocity  $v_{SL} \approx v_{NL}/S$  and a transit time  $\tau_{SL} = LS/v_{NL}$ , where  $S$  is the slow down factor [21]. Using the pulse delay  $\tau_D$  of 1 ps, we thus have  $\tau_{SL} \approx 3.81$  ps, and a modest  $S$  value  $\sim 1.4$ , corresponding to  $v_{SL} \sim 0.48 c$ .

Further increase in the tilt angle brings the laser too close to the band-edge, and results in greatly diminished transmission of the slow pulse which also likely experiences severe pulse broadening effect [17] due to steepening of the group velocity dispersion, c.f. Fig. 1(b); consequently, we detect only a very weak and broad SFG signal for  $\theta > 7^\circ$ , i.e. no pulse separation. An interesting and intriguing observation is made if we use CLC-1 at a tilt angle  $\theta > 16^\circ$  or CLC-2 at normal incidence, cf. Figure 3(b) and 4(b), when the laser wavelength is located *inside* the photonic bandgap. In this case, a pulse of similar pulse duration as the NL pulse but smaller in amplitude is detected at a time delay of  $\sim 11$  ps, implying the slow-down of the group velocity to  $v_{SL} \sim 0.13c$ . While one can clearly rule out band-edge dispersion effect, the underlying mechanism remains unclear at present.

#### 4. Summary

In conclusion, we have demonstrated several significant breakthroughs in the study of cholesteric liquid crystal for ultrafast photonic operations. The development of FASA technique has enabled routine fabrication of very thick good optical quality planar aligned CLC cells that exhibit desirable photonic crystal properties. By probing the cell with linearly polarized 600 fs laser pulse, we have observed pulse separation of  $\sim 1$  ps between the NL and SL pulses due to group velocity dispersion at the photonic band-edge. Much larger effects will manifest with optimization in the materials/optical parameters such as laser pulse duration and optimized band-edge/laser wavelength location. In conjunction with previous successful demonstration of compression, stretching and recompression of femtosecond laser pulses, these  $\sim$ mm thick CLC cells thus present themselves as highly promising compact, all-optical and versatile alternative to current state-of-the-art materials/devices for slow-light and ultrafast laser pulse modulation.

**Funding**

Air Force Office of Scientific Research (FA9550-14-1-0297).

**Acknowledgments**

Sin-An Lin assisted in the initial preparation of CLC sample.